AN EXPERIMENTAL STUDY OF THE VIBRATIONAL CHARACTERISTICS OF A DIAMOND CIRCULAR BLADE USING ELECTRONIC SPECKLE-PATTERN INTERFEROMETRY AND FEM

Mykhaylo TKACH[*], Yurii HALYNKIN[*], Arkadii PROSKURIN[*], Irina ZHUK[**] , Volodymyr KLUCHNYK[*] , Igor BOBYLEV[*]

[*] Department of Engineering Mechanics and Technology of Marine Engineering, Engineering and Research Institute of Engineering, Admiral Makarov National University of Shipbuilding, Mykolaiv, 9 Heroes of Ukraine Avenue, Ukraine
[**]Department of Automation and Computer-Integrated Technologies, Faculty of Computer Science, Petro Mohyla Black Sea National University, Mykolaiv, street 68 Desantnikov 10, Ukraine

mykhaylo.tkach@nuos.edu.ua, yurii.galynkin@nuos.edu.ua, arkadii.proskurin@nuos.edu.ua, iryna.zhuk@chmnu.edu.ua, vladimir.kluchnyk@gmail.com, igor.bobylev.nuk@gmail.com

received 13 March 2020, revised 10 March 2021, accepted 13 March 2021

Abstract: The compact installation and technology for determining vibration characteristics by the ESPI method has been created. The experimental determination of the dynamic characteristics of a diamond circular blade with a diameter of 203.4 mm and a thickness of 1.19 mm using real-time electronic speckle interferometry is presented. 15 mode shapes of vibration were detected in the range from 100 to 5000 Hz. The program calculation of the natural frequencies and mode shapes is carried out for three values of the clamping inner diameter (42 mm, 44 mm, 46 mm). The options for calculating a disk with a rim and without a rim are considered. It is shown that the minimum mean squared error of the calculation is achieved for the values of the diameter of the disk 46 mm, 42 mm and 44 mm for the number of nodal circles 0, 1 and 2, respectively. To verify the accuracy of the interferometer, experimental, computational and analytical studies of console steel rod 200 x 22.25 x 3.78 mm in size were carried out.

Key words: interferometry, speckle pattern, correlation fringes, vibrational analysis

1. INTRODUCTION

Modern engineering is characterized by an increase in the specific capacities of machines and devices. During operation, cutting wheels and circular saws rotate at high frequencies and are subject to significant dynamic loads. The resulting resonant vibration significantly increases the loads on them and on the bearings. This is one of the main reasons for the breakdown of such a tool. Also, the roughness of the processed surface increases and the service life of the equipment decreases.

The solution to the problems of the strength of parts under dynamic loads is one of the most complex and time-consuming. These conditions determine the relevance of studies of vibrational characteristics of disk structural elements both at the stage of design and development of products, and in the analysis of emergency situations.

The creation of structures operating under vibrational loads and the implementation of measures for detuning from resonance involves, first of all, determining the spectrum of resonant frequencies and vibration mode shapes. Moreover, the results of the study of the dynamic parameters of a homogeneous disk clamped in the center (on the shaft) are of independent importance and can serve as a reference point in the study of oscillations of the disks of turbomachines (Levin, 1953).

Determination of natural frequencies and vibration modes of solids can be carried out by a theoretical, experimental or theoretical-experimental method. The first practical method for visualizing vibration modes on plates and, therefore, for conducting an experimental analysis of vibration, was invented by Chladni in the 1780s (Chladni and Beyer, 2015). The method includes spraying a fine powder, such as sand, onto the surface of the plate, so it is not a non-contact method. In the book Wailer (1961), studies of round, elliptical, rectangular and other polygonal plates are presented, as well as practical and historical notes. The results include extensive graphical tables of observed mode forms, a method for classifying mode forms, and a discussion of how these forms arise. The ESPI method was used to experimentally test analytical and numerical models of applied mechanics in Halama et al., (2016), vibration theory in Chi-Hung et al., (2004), in the automotive industry by Beeck and Hentschel (2000) as well as Van der Auweraer et al., (2002), materials science in Richardson et al., (1998), biomedical field by Yang et al., (2014), microelectromechanical systems in an article by Foitzik et al., (2003) and in many other areas of science and technology. A detailed study of the frequencies and modes of vibrations of a solid homogeneous disk fixed in the center was carried out by Makaeva et al., (2008a), (2008b). Experimental studies were carried out by the method of holographic interferometry (Makaeva et al. 2008a).

The Rayleigh – Ritz method provides numerical determination of approximate values of frequencies and natural forms of resonant vibrations (Babakov, 1965). Therefore, in engineering practice, the theoretical calculation of the resonant parameters of structures is mainly performed numerically by the finite element method (Mrozek et al. 2018), implemented in modern software systems ANSYS, NASTRAN, COSMOS, FEMAP, etc.

But the errors in modelling the boundary conditions, the mis-

match of the calculation model with the object of study reduce the reliability of the calculated data and almost always require their experimental verification.

To study the vibration characteristics of the disk, the method of electronic speckle-pattern interferometry was used. With a good quality of interferograms, it ensures the automation of experimental research reduces the requirements for vibration isolation of stands and eliminates the need for photochemical processing.

In addition, a highly accurate experimental determination of vibration parameters is crucial for the implementation of the combined calculation and experimental method, when the experimental data are used to form boundary conditions, and the numerical method is used for a detailed analysis of the distribution of amplitudes, deformations, and stresses in the entire volume of the studied object. It allows to increase the accuracy and reduce the complexity of determining the dynamic parameters of disk-shaped parts of machines and mechanisms (Careva and Tupoleva, 2006).

Therefore, this work devoted to the creation of an experimental stand and the conduct of a comprehensive experimental and numerical study of the natural frequencies and modes of vibration clamped in the center of the disk is relevant.

2. THEORETICAL PART

2.1. Description of the interferometric stand

In experimental mechanics, non-contact optical methods are used to study the vibrations of solids, which use the coherent properties of laser radiation.

The most informative is the method of holographic interferometry (HI) (Vest, 1982). It makes it possible in real time to visualize the dislocation of nodal lines i.e. determine the mode shapes and the value of the resonant frequency. The resolution of holographic interferograms makes it possible to estimate with high accuracy the distribution of vibration amplitudes over the surface of an object. But the technique for obtaining holographic interferograms is rather complicated, involves the use of photographic plates with the need for their accurate positioning and photochemical processing, good vibration protection of the optical stand and highly coherent laser radiation. Almost the same completeness of information about the vibrational process, but lower resolution of interference fringes, has the electron speckle-pattern interferometry (ESPI) method (Jones and Wykes, 1989).

With less stringent requirements for the experimental technique and less laboriousness, it allows you to quickly determine the resonant frequency and observe the form of vibrations on a computer screen in real time without using the photochemical process. It is indispensable in the case of serial control of products, if necessary, an express analysis. This determined our choice of research method.

The contrast of the bands on speckle interferograms obtained using an interferometer with a speckle-modulated reference wave is, other things being equal, lower than on interferograms with a smooth reference wave (Yelenevsky and Shaposhnikov, 2001) (Zhuzhukin, 2011). But the optical design of such an interferometer is rather cumbersome, extremely difficult to align and requires periodic monitoring due to its low resistance to external disturbances. In this work, an extremely simple optical scheme of a digital speckle interferometer with combined beams was proposed, which has increased noise immunity. But the use of a large-sized transmitting diffuser with precision movement, which is larger than the object of study in size, does not allow creating a compact portable device (Zhuzhukin, 2011).

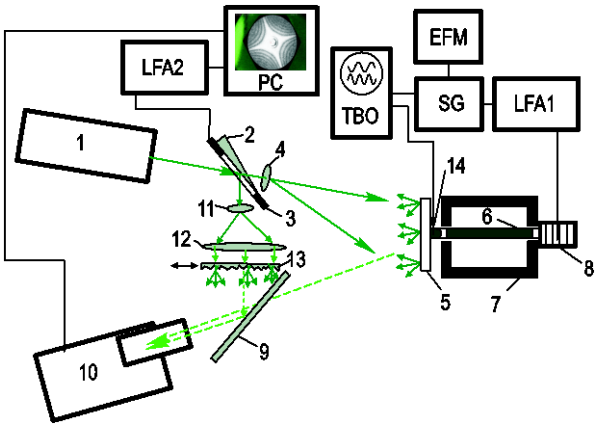

Fig. 1. Optical design and hardware of the ESPI stand: 1 - laser, 2 - optical wedge, 3 - piezoceramic ring, 4,11 - micro lens, 5 - test disk, 6 - mounting pin, 7 - clamp case, 8 - piezoceramic vibrator, 9 - beam splitter, 10 - video camera, 12 - collecting lens, 13 - diffuser, 14 - bimorph vibration sensor, SG - sound generator, TBO - two-beam oscilloscope, EFM - electronic frequency meter, PC - personal computer, LFA 1 , LFA 2 - low frequency amplifiers

In our studies, we used an interferometer with a diffuse reference wave and separated branches. Such a compromise solution made it possible to create a mobile compact electronic speckle-pattern interferometer with satisfactory noise immunity, sufficient to conduct vibration diagnostics of products outside the bench environment (Petrov and Lau, 1995).

The optical design and hardware of the created digital signal center are presented in Fig. 1. A coherent light source is a solid-state DPSS laser 1 with a radiation power of 50 mW and a wavelength of $\lambda = 0.532$ μm. The laser beam by an optical wedge 2 is divided into transmitted and reflected, forming channels of the subject and reference beams. The transmitted beam is expanded by a micro lens 4, scattered by the matte surface of the investigated disk 5, and creates a diffuse object wave. Passing through the beam splitter 9, it is focused by the lens of the video camera 10 on the plane of the charge-coupled device (CCD) as an object speckle field.

The beam reflected from the beamsplitting wedge is expanded by the micro-lens 11, collimated by the lens 12 and scattered by the transmitting diffuser 13, forming a diffuse reference wave. On the beam splitter 9, it is combined with the subject and, after refraction in the camera lens, forms a speckle reference field on the matrix surface (Mihaylova et al. 2004), (Mihaylova et al. 2006). The contrast of the resulting speckle pattern will be maximum at the same average intensities and consistent polarizations of the interfering beams. To avoid depolarization of radiation, the diffuser 13 is thin surface etched (Vest, 1982), and aluminum powder is used to paint the disk. The intensity equalization is carried out by changing the intensity of the reference wave when moving the lens 12.

Due to the compact arrangement of the interferometer, the optical path lengths of the reference and subject speckles differ by an order of magnitude. The mismatch in the curvature of the interfering wave fronts leads to a certain decrease in the amplitude of the useful signal (Gorbatenko et al. 2001). But the operating experience of the installation showed that a noticeable deterioration in the quality of the interferogram is not observed.

Video camera 10 operates in the webcam mode and real-time transmits a video stream of 25 frames per second to a computer with a resolution of 720x576 pixels with a brightness division into 256 gradations. To match the spatial frequency of the resulting speckles with the resolution of the CCD matrix, aperture the lens aperture to the value F = 16 ... 22. At the same time, the frame registration time τ was in the range 0.01 - 0.02 s. A detailed description of the methods for obtaining and processing holographic information is given by the authors in (Tkach et al. 2020), (Tkach et al. 2021).

In this work, we used a diamond circular blade 5 (Fig. 2) with a diameter of 203.4 ± 0.05 mm and a thickness of 1.19 ± 0.05 mm; in addition, there is a rim with a width of 5 ± 0.05 mm and an outer edge of the diamond circular blade 1.57 ± 0.05 mm thick. The diamond circular blade is clamped using two faceplates with a diameter of 46 mm mounted on a threaded rod 6 with a diameter of 27 mm, which is an analog of the shaft. To simulate the operational boundary conditions for mounting the shaft, the pin is clamped at two points in the massive casing 7 (Fig. 3) with an internal cavity. The second end of the stud abuts against the pusher of the piezoceramic vibro-column 8, to which a sinusoidal signal of the sound generator (SG) is fed, previously amplified by the amplifier LFA 1. The elastic wave from the vibrator is transmitted to the stud and excites vibration of the disk under study. Such a wave excitation method eliminates the influence of the attached mass of the vibrator on the disk vibrations.

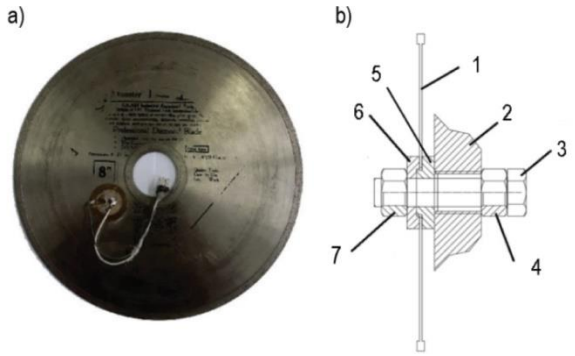

Fig. 2. a) Test diamond circular blade, b) Drawing of the diamond circular blade in the fixture. 1 - diamond circular blade, 2 - clamping case, 3 - threaded rod, 4, 7 - bolts, 5,6 - pressure washer

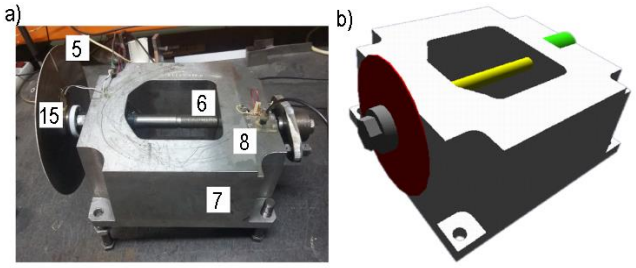

Fig. 3. a) Test drive clamping pattern, b) 3D Test drive clamping model: the disc is highlighted in red, the stud is yellow, the ceramic piezo washers are green

The frequency multiplicity of the disk oscillation frequency relative to the frequency of the SG signal was controlled using a small-sized bimorph vibration sensor 15 glued to the disk at the pinch boundary. The frequency of the vibration excitation signal is measured by the electronic frequency counter of the EFM, and the generator signal is compared with the vibration sensor signal by a two-beam TBO oscilloscope.

2.2. ESPI method basics

Electronic speckle interferometry refers to non-contact laser measuring instruments and, like holographic interferometry, allows for resonant vibration of a part to determine the dislocation of nodal lines along its entire surface (Levin, 1953). The experimental technique and the method for producing interferograms are described in more detail in the original sources: (Mrozek et al. 2018); (Jones and Wykes, 1989); (Yelenevsky and Shaposhnikov, 2001); (Zhuzhukin and Solyannikov, 2014); (Komarov, 2004); (Bystrov and Zhuzhukin, 2017); (Tkach et al. 2012); (Tkach et al. 2015).

When performing these studies, the method for determining the resonance frequencies of a disk by speckle interferometry is to place the disk in a clamping device, excite oscillations of the disk at resonant frequencies, register the speckle interferogram in real time, by analyzing the signal from the camera, and determine vibrating speckles based on this information (Babakov, 1965).

This allows you to fundamentally reduce the time of research of the dynamic parameters of the object and improve the visualization and image of the waveform using computer processing.

3. EXPERIMENTAL PART

3.1. Experimental determination of natural frequencies and mode shapes of a diamond circular blade

The resonant frequencies and the corresponding lateral vibrations of the diamond circular blade were obtained using the laboratory bench described in Section 2.1. The thickness of the diamond circular blade with a diameter of 203.4 ± 0.05 mm was measured at twenty different points (Fig. 4). The measurement results are shown in Tab. 1. According to these measurements, the average circle thickness was calculated, which amounted to 1.19 ± 0.05 mm, as well as the average rim thickness of 1.57 ± 0.05 mm. In the experiment, the circle was clamped using two faceplates.

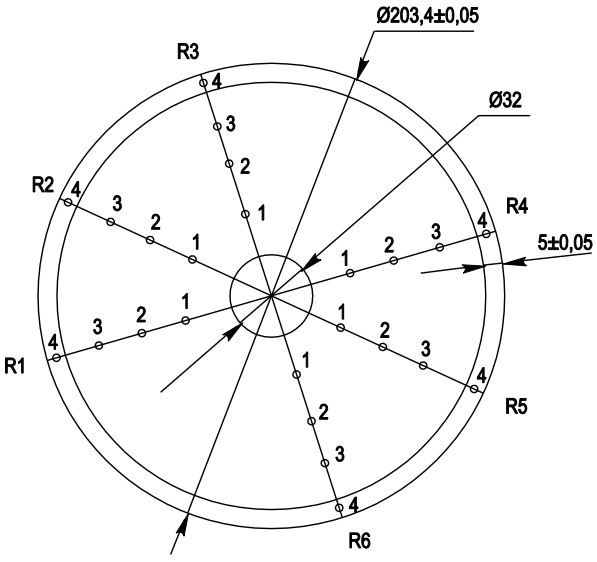

Fig. 4. Diamond circular blade measurement circuit

DOI 10.2478/ama-2021-0003

Tab. 1. Diamond circular blade thickness measurement results

Diam-eter (mm)	Point	R1	R2	R3	R4	R5	R6
50	1	1.22	1.21	1.22	1.19	1.22	1.22
100	2	1.16	1.17	1.16	1.16	1.17	1.16
150	3	1.20	1.18	1.17	1.21	1.21	1.22
200	4	1.59	1.57	1.56	1.54	1.59	1.56

A number of characteristic forms of vibrations obtained as a result of the experiment are presented in Tab. 2 and Fig. 5.

Tab. 2. Experimental mode shapes and natural frequencies of a diamond circular blade

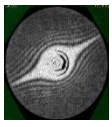	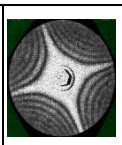	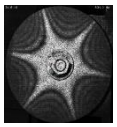	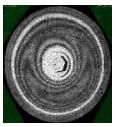	
153 Hz	200 Hz	377 Hz	944 Hz	980 Hz
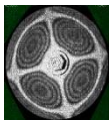	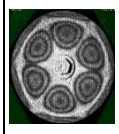	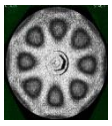	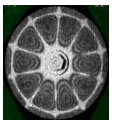	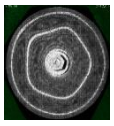
1184 Hz	1543 Hz	2049 Hz	2669 Hz	2851 Hz
	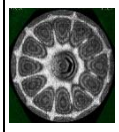	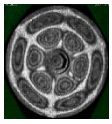		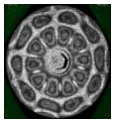
3026 Hz	3376 Hz	3471 Hz	4120 Hz	4932 Hz

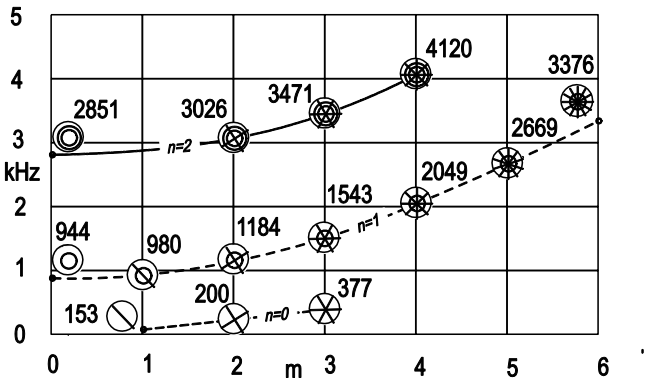

Fig. 5. Experimental values of the natural frequencies of the diamond circular blade; n - the number of nodal circles, m - the number of nodal diameters

In addition, we revealed mode shapes (Fig. 6), similar to those found in the work of E. Chladni Treatise on Acoustics (Chladni and Beyer, 2015) under number 109b.

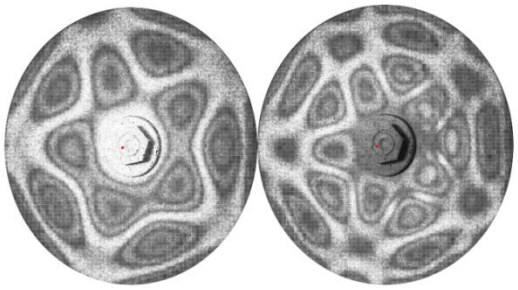

Fig. 6. Mode shapes similar to form 109b (Chladni and Beyer, 2015)

3.2. Calculation of natural frequencies and mode shapes of a diamond circular blade by the finite element method

Using the ANSYS Workbench software, we obtained resonant frequencies and the corresponding lateral vibrations of the circular blade. For this, a 3D model of a circular blade was created, the measurements of which are described in section 3.1. The boundary conditions in the calculation were: the disk was clamped along the inner diameter and free at its outer diameter. This corresponds to the fastening of the disk on the experimental stand in Fig. 2 (b).

For the calculation, a SOLID 186 finite element (tetrahedron) with a size of 0.595 mm was used. The total number of elements was about 400 thousand as shown in Fig. 7. Calculations performed with a twofold decrease in the size of the finite element did not reveal a significant change in the frequencies and vibration modes of the disk under study.

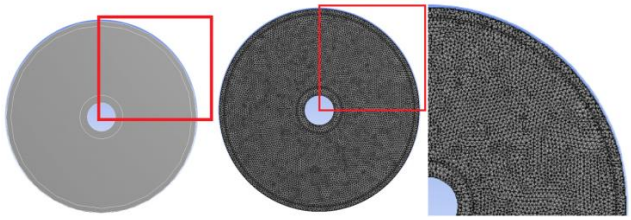

Fig. 7. 3D model of a diamond circular blade and its breakdown into tetrahedra

Tab. 3. Mode shapes and natural frequencies of a diamond circular blade obtained by calculation

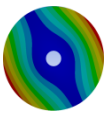	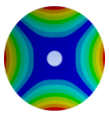	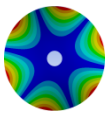	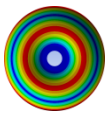	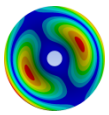
139 Hz	187 Hz	364 Hz	931 Hz	994 Hz
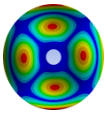	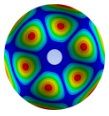	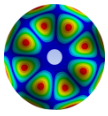	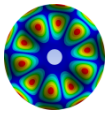	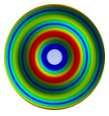
1204 Hz	1583 Hz	2113 Hz	2756 Hz	2713 Hz
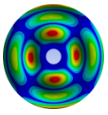	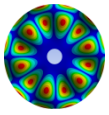	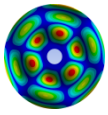	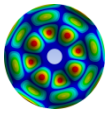	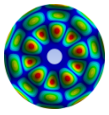
3049 Hz	3484 Hz	3508 Hz	4178 Hz	5033 Hz

The type of material chosen for the calculation is structural steel. Material properties: density - 7.81 g / cm3, Young's modulus - 200 GPa, Poisson's ratio - 0.28. A number of characteristic forms of oscillations obtained as a result of program calculation are presented in Tab. 3.

In addition, using the ANSYS Workbench software, a calculation was made of the natural frequencies and vibration modes for different clamping diameters of the diamond circular blade. For greater accuracy, the calculation was carried out taking into account the rim of the diamond circular blade, as well as without it. The results are presented in Tab. 4 and Tab. 5.

Tab. 4. Experimental and calculated values of the natural frequencies of the diamond circular blade without taking into account the rim

Experiment, Hz	Calculation of fixing diameter 42mm, Hz	Calculation of fixing diameter 44mm, Hz	Calculation of fixing diameter 46mm, Hz
153.0	139.0	143.0	148.0
200.0	187.0	191.0	194.0
377.0	364.0	365.0	366.0
944.0	931.0	956.0	981.0
980.0	994.0	1019.0	1044.0
1184.0	1204.0	1225.0	1246.0
1543.0	1583.0	1596.0	1610.0
2049.0	2113.0	2119.0	2125.0
2669.0	2756.0	2757.0	2760.0
2851.0	2713.0	2785.0	2857.0
3026.0	3049.0	3113.0	3177.0
3376.0	3484.0	3485.0	3485.0
3471.0	3508.0	3558.0	3610.0
4120.0	4178.0	4209.0	4244.0

Tab. 5. Experimental and calculated values of the natural frequencies of the diamond circular blade, taking into account the rim

Experiment, Hz	Calculation for clamping diameter 42mm, Hz	Calculation for clamping diameter 44mm, Hz	Calculation for clamping diameter 46mm, Hz
153.0	134.0	139.0	143.0
200.0	186.0	189.0	192.0
377.0	373.0	374.0	375.0
944.0	911.0	935.0	959.0
980.0	977.0	1000.0	1023.0
1184.0	1192.0	1212.0	1231.0
1543.0	1577.0	1590.0	1602.0
2049.0	2117.0	2123.0	2126.0
2669.0	2773.0	2775.0	2773.0
2851.0	2667.0	2735.0	2802.0
3026.0	3016.0	3076.0	3134.0
3376.0	3519.0	3519.0	3515.0
3471.0	3488.0	3536.0	3581.0
4120.0	4173.0	4204.0	4231.0

4. RESULTS

A graph of the results of the experiment is given (Fig. 5), as well as graphs of the errors in calculating various diameters of fastening the diamond circular blade (Fig. 8).

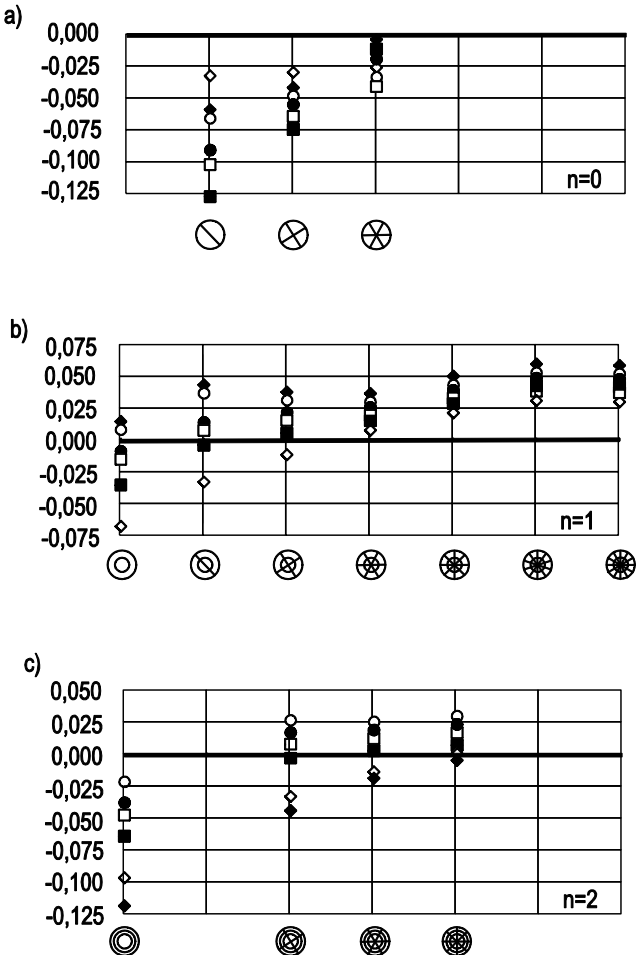

Fig. 8. The relative error of the calculated for clamping diameters of the diamond circular blade relative to the experiment; where number of modal circles is, a) n = 0, b) n = 1, c) n = 2; ● - Ø44 with a rim, ○ - Ø44 without a rim, ◆ - Ø46 with a rim, ◇ - Ø46 without a rim, ■ - Ø42 with a rim, □ - Ø42 without a rim.

The ratios of the experimental and calculated program frequencies are relatively equal (Table 5), therefore, the difference between them is caused by the difference in geometry between the analytical and real circular blades (Joenathan et al. 1995), (Qin et al. 2016) and the incorrectly selected material property for program calculation.

The value of the mean squared error of the program calculation of frequencies for different clamping diameters of the diamond circular blade, as well as for a different number of nodal circles, is presented in Tab. 6.

Tab. 6 The root mean squared error of the calculation of frequencies, for the n=0, n=1 and n=2 respectively

n=0	⌀42	⌀44	⌀46
With rim	0,0825	0,0619	0,0444
Without rim	0,0678	0,0493	0,0311

n=1	⌀42	⌀44	⌀46
With rim	0,0295	0,0309	0,0375
Without rim	0,0253	0,0327	0,0447

n=2	⌀42	⌀44	⌀46
With rim	0,0331	0,0265	0,0287
Without rim	0,026	0,0245	0,0353

5. VERIFICATION OF EXPERIMENTAL STAND

5.1. Experimental determination of natural frequencies and mode shapes of a rectangular rod

To test the operability, as well as the serviceability of the experimental bench, tests were carried out in advance of a rectangular steel rod. The rod material is carbon steel 45. Rod dimensions: length - 240 mm, width - 22.25 ± 0.21 mm, thickness - 3.78 ± 0.03 mm.

To carry out the experiment, the lower part of the rod clamped by two plates in the clamp; the upper part is free. The length of the free oscillating console part of the rod is 200 mm and clamped part is 40 mm. The size of the plates used for clamping the rod is: length - 50 mm, width - 50 mm, thickness – 20 mm.

A number of characteristic waveforms obtained from the tests are presented in Tab. 7.

Tab. 7. Experimental natural frequencies and mode shapes of a rectangular rod

	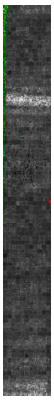	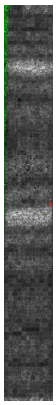	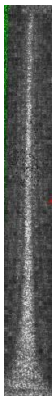	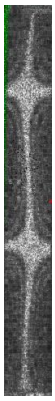	
71 Hz	447 Hz	1209 Hz	1246 Hz	6392 Hz	9051 Hz

5.2. Calculation of natural frequencies and mode shapes of a rod of rectangular cross section by the finite element method

Using the ANSYS Workbench software, we obtained resonant frequencies and the corresponding vibration modes of a rectangular rod. For this, a 3D model of the rod was created, the properties, type, and clamping scheme of which are described in Section 5.1. For calculation, the 3D model was divided into individual cubic elements, (about 400 thousand) and is shown in Fig. 9. The element type used in the calculation is SOLID186; the element size is 1 mm. The boundary conditions: clamping for down side and free at three sides.

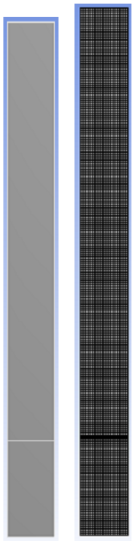

Fig. 9. 3D model of the rod and its division into finite elements

The type of material chosen for the calculation is structural steel. Material properties used in the calculation: density - 7.81 g / cm3, Young's modulus - 200 GPa, Poisson's ratio - 0.28.

A number of characteristic forms of oscillations obtained as a result of program calculation are presented in Tab. 8

Tab. 8. Natural frequencies and mode shapes of the rod obtained in the ANSYS program

	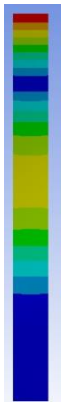	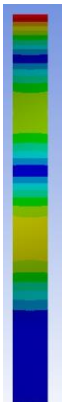	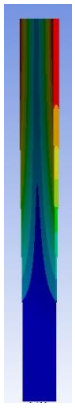	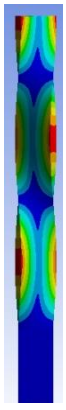	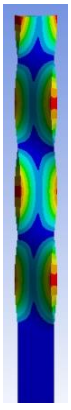
77,5 Hz	485,2 Hz	1356,1 Hz	1274,7 Hz	6480,5 Hz	9217,4 Hz

5.3. Comparison of the results of calculating the natural frequencies and mode shapes of a rod of rectangular cross section

A comparison of the frequencies of the resonant vibrations of the rod obtained experimentally, analytically and using the finite element method is shown in table. 9. The analytical calculation was carried out using the Euler–Bernoulli beam theory (Babakov, 1965).

Tab. 9. Comparison of the results of an experimental study and calculation of a rod

Mode shape		The experimental frequency, Hz	Calculation, Hz	
Torsional	Flexural		FEM	Analytical
0	1	71	77	77.8
0	2	447	485	482.5
0	3	1209	1356	1370.5
1	0	1246	1274	1244.7
1	2	6392	6480	6223.4
1	3	9051	9217	8712.7

6. CONCLUSIONS

A stand has been created to determine the natural frequencies and mode shapes using real-time electronic speckle-pattern interferometry.

An experimental study of the natural frequencies and mode shapes of a diamond circular blade was carried out using real-time electronic speckle-pattern interferometry. 15 mode shapes of the diamond circular blade were revealed in the frequency range from 100 to 5000 Hz.

A programmatic calculation of the natural frequencies and mode shapes by the finite element method for three diameters of fastening the diamond circular blade was made.

The experimental results are compared with the calculated ones, the mean squared error and an error analysis is also carried out.

To test the operability, as well as the serviceability of the experimental bench, tests and calculations of a rectangular steel rod were carried out.

REFERENCES

1. **Babakov I.M.** (1965), *Theory of vibrations* [Teorija kolebanil], Science [Nauka]. [In Russian]
2. **Beeck M.A., Hentschel W.** (2000), Laser metrology - a diagnostic tool in automotive development processes, *Optics and Lasers in Engineering*, 34(2), 101–120.
3. **Bystrov, N. D., Zhuzhukin, A. I.** (2017), Speckle Interferometry in the Investigation of Large-Size Turbine Engine Structures Vibration, *Procedia Engineering*., 176: 471–475.
4. **Careva A.M., Tupoleva A.N.** (2006), *Application of an experimental calculation method for determining resonant frequencies and vibration modes of a disk of constant thickness* [Primenenie eksperimentalno-raschetnogo metoda dlya opredeleniya rezonansnyh chastot i form kolebanij diska postoyannoj tolshiny], Kama State Academy of Engineering and Economics [Kamskaya gosudarstvennaya inzhenerno-ekonomicheskaya akademiya]. [In Russian]
5. **Chi-Hung H., Yu-Chih L., Chien-Ching M.** (2004) Theoretical analysis and experimental measurement for resonant vibration of piezoceramic circular plates, *IEEE Transactions On Ultrasonics, Ferroelectrics, And Frequency Control*, 51(1), 12-24.
6. **Chladni. E., Beyer T.** (2015), *Treatise on Acoustics*, Springer International Publishing Switzerland.
7. **Foitzik A.H., Kaese W., Vogt T., Sommerer M., Arkhipov S.** (2003), Static and Dynamic Characterization of MEMS via ESPI, *International Journal Of Computational Engineering Science*, 4(3), 467–470.
8. **Gorbatenko B.B., Lyakin D.V., Perepelitsyna O.A., Ryabukho V.P.** (2001), Optical schemes and statistical properties of displacement speckle interferometer signal [Opticheskie shemi I statisticheskie harakteristiki signala spekl-interferometrov peremeshenij], C*omputer optics* [Kompyuternaya optika], tom 33, №3. [In Russian]
9. **Halama R., Hornacek L., Pecenka L., Krejsa M., Smach J.** (2016), 3-D ESPI Measurements Applied to Selected Engineering Problems, *Applied Mechanics and Materials*, 827, 65–68.
10. **Joenathan C., Sohmer A., Burkle L.** (1995), Increased sensitivity to in-plane displacements in electronic speckle pattern interferometry, *Appl. Opt.*, Vol. 34, No.16, 2880-2885
11. **Jones R., Wykes C.** (1989), *Holographic and Speckle Interferometry*. 2 edition, Cambridge University Press.
12. **Komarov Yu.S.** (2004), *Noise-resistant digital speckle interferometer for vibrometry of objects based on the method of averaging over time* [Pomehoustojchivyj cifrovoj spekl-interferometr dlya vibrometrii obektov na osnove metoda usredneniya vo vremeni], Abstract of dissertation for the degree of candidate of technical sciences [Avtoreferat dissertacii na soiskanie uchenoj stepeni k.t.n]. [In Russian]
13. **Levin A.V.** (1953), *Working Blades and Disks of Steam Turbines* [Rabochije lopatki I diski parovyh turbin], Gosenergoizdat [Gosenergoizdat]. [In Russian]
14. **Makaeva R.Kh., Tsareva A.M., Karimov A.Kh. (**2008), Determination of natural frequencies and forms of vibrations of the disk of constant thickness, fixed in the center // Izv. vuzov. *Aviation technique*, No 1 - C. 41 - 45.
15. **Makaeva R.Kh., Tsareva A.M., Karimov A.Kh. (**2008), Determination of natural frequencies and vibration modes of a constant thickness centrally secured disk. *Russ. Aeronaut.* **51,** 53–59 (2008).
16. **Mihaylova E., Naydenova I., Martin S., Toal V.** (2004), Electronic speckle pattern shearing interferometer with a photopolymer holographic grating, *Appl. Opt.*, Vol. 43, No. 12, 2439-2442.
17. **Mihaylova E., Naydenova I., Martin S., Toal V.** (2006), Photopolymer diffractive optical elements in electronic speckle pattern shearing interferometry, *Opt. Lasers Eng*., Vol. 44, No. 9, 965-974.
18. **Mrozek P., Mrozek E., Werner A.** (2018), Electronic speckle pattern interferometry for vibrational analysis of cutting tools, *Acta Mechanica et aAutomatica*, vol 12, no.2.
19. **Petrov V., Lau B.** (1996), Electronic speckle pattern interferometry with a holographically generated reference wave," *Opt. Eng*. Vol. 35, No. 8, 2363-2370.
20. **Qin J., Gao Z., Wang X., Yang S.** (2016), Three-Dimensional Continuous Displacement Measurement with Temporal Speckle Pattern Interferometry, *Sensors*, (Basel, Switzerland).
21. **Richardson M.O.W., Zhang Z.Y., Wisheart M., Tyrer J.R. Petzing J.** (1998), ESPI non-destructive testing of GRP composite materials containing impact damage, *Composites* Part A, 29A, 721–729.
22. **Tkach M. et al.** (2021*)* Improving the Noise Immunity of the Measuring and Computing Coherent-Optical Vibrodiagnostic Complex, In: Nechyporuk M., Pavlikov V., Kritskiy D. (eds) Integrated Computer Technologies in Mechanical Engineering - 2020.

ICTM 2020, *Lecture Notes in Networks and Systems*, vol 188. Springer, Cham.
23. **Tkach M.R., Zolotiy Yu.G., Dovgan D.V., Guk I.Yu.** (2012), Determination of the natural vibration forms of gas turbine engine elements in real time by electron speckle interferometry [Opredelenie form sobstvennih kolebanij elementov GTD v realnom vremeni metodom electronnoj spekl-interferometrii], *Aerospace technic and technology* [Aviacionno-kosmicheskaya tehnika i tehnologiya] № 8 (95). [In Russian]
24. **Tkach M.R., Zolotiy Yu.G., Dovgan D.V., Guk I.Yu.** (2015), *Patent: Method of determining of forms of resonant vibrations shapes of blades of gas turbine engine by speckle interferogram*, UA 103068. [In Ukrainian]
25. **Tkach, M., Morhun, S., Zolotoy, Y., Zhuk, I**. (2020), Modal analysis of the axial compressor blade: advanced time-dependent electronic interferometry and finite element method, *Int. J. Turbo Jet-Eng.*
26. **Van der Auweraer H., Steinbichler H., Vanlanduit S., Haberstok C., Freymann R., Storer D., Linet V.** (2002), Application of stroboscopic and pulsed-laser electronic speckle pattern interferometry (ESPI) to modal analysis problems, *Measurements Science and Technology*, 13, 451–463.
27. **Vest. C. M.** (1982), *Holographic Interferometry*, John Wiley and Sons, New York.
28. **Wailer, M.D.**, (1961), *Chladni Figures: a Study in Symmetry*, G. Beil & Sons (London).
29. **Yang L., Xie X., Zhu L., Wu S., Wang Y.** (2014), Review of Electronic Speckle Pattern Interferometry (ESPI) for Three Dimensional Displacement Measurement, *Chinese Journal Of Mechanical Engineering*, 27(1), 1–13.
30. **Yelenevsky D.S., Shaposhnikov Yu.N.** (2001), *Investigation of acoustic emission procession of the structures through electronic speckle interferometry methods* [Issledovanie processov zvukoizluchenia konstrukcij metodami elektronnoj spekl-interferometrii], Izvestiya of the Samara Science Centre of the Russian Academy of Sciences [Izvestiya Samarskogo Nauchnogo Centra Rossijskoj Akademii Nauk]. [In Russian]
31. **Zhuzhukin A.I.** (2011), A mobile speckle interferometer for studying vibration modes of vibrating objects outside bench conditions [Mobilnyj spekl-interferometr dlya issledovaniya form kolebanij vibriruyushih obektov vo vne stendovyh usloviyah], *Electronic journal* «Trudy MAI» [Elektronnyj zhurnal «Trudy MAI»] № 48. [In Russian]
32. **Zhuzhukin A.I., Solyannikov V.A.** (2014), *Method of reducing speckle-interferometer sensitivity for the study of turbomachine elements vibration* [Metod umensheniya chuvstvitelnosti spekl-interferometra pri issledovanii vibratsii detalej turbomashin], *Vestnik of Samara University: Aerospace and Mechanical Engineering* [Vestnik Samarskogo gosudarstvennogo aerokosmicheskogo universiteta] № 1(43). [In Russian]